Interface Structure and Surface Polarity in CdTe/ZnTe/(112)Si Hetero-Epitaxial System

N. K. Dhar
Army Research Laboratory
2800 Powder Mill Road, Maryland 20783-1197
email: ndhar@arl.mil

ABSTRACT

Tellurium adsorption on clean (112) Si surfaces obey a second order kinetic law. The adsorbed Te ad-atoms are highly immobile. Activation energies of adsorption and desorption were measured by isothermal desorption rates. A surface bond energy model was used to calculate the total energy for Te chemisorption on (111) terraces. This model yields a Si-Te bond energy of about 3.46 eV. As-Te bond energy was found to be about 4.0 eV. ZnTe/CdTe epitaxy on As-passivated Si gave uniform and smooth surfaces. As-pasivated surfaces always produced B-type CdTe crystallographic polarity. Te coverage on As-passivated surfaces were significantly lower than the coverage observed on clean Si surfaces. A ZnTe nucleation model is proposed suggesting an enhancement in Te surface mobility occurs on As-passivated surfaces. ZnTe nucleation on As-passivated surfaces initiates at the step edges. ZnTe/CdTe epitaxy on Te-terminated Si and directly on clean (112) Si produced rough surface morphology. The surface polarity type depended on the initial Si surface preparation. A B-type polarity is observed for surfaces treated with Te at temperatures above 500º C. For Te adsorption temperatures below 450º C, CdTe surfaces were A-type and heavily faceted. ZnTe growth on Te-terminated surfaces is suggested to initiate mainly from nucleating on the terraces.

I. Introduction

Si as a substrate for HgCdTe infrared detector array has many advantages. In recent years many reports appeared on this subject, particularly on the issue of CdTe growth on Si substrates [1-3]. Even though B-type CdTe layers with etch pit density (EPD) in the order of 10^5 cm^{-2} can now be achieved, the frequent occurrence of surface polarity conversion to A-type with high density of surface facets, and the nature of the interface structure is not understood. Low EPD values have been possible because of the Si surface preparation with As and the use of a thin ZnTe layer at the interface [4]. Therefore, an understanding of the ZnTe nucleation on Si, and the nature of the interface structure is of interest.

Nucleation of ZnTe and CdTe on “atomically clean” (112)Si substrates initiate by the formation of Si-Te bonds at the interface. This is expected because sticking coefficient of Te at typical growth temperatures is unity and Zn or Cd tends to stick on Si surfaces only when Te is present. The kinetics of Te adsorption on Si surfaces is of interest because the properties of the subsequent ZnTe/CdTe growth, such as surface crystallographic polarity, is typically influenced by the nature of the Si-Te bonding at the initial stages of growth.

Studies of Zn and Te adsorption on As-passivated Si surfaces suggest that Zn sticking probability is negligible. Te sticking probability is significantly lower than it is on "atomically clean" Si surfaces. In this paper, kinetics of Te adsorption on (112) Si surfaces is treated using the transition state theory. Desorption isotherms were measured to determine the absolute rate constants and the bond energies of Te on "atomically clean" (112) surfaces. RHEED, Temperature Programmed Desorption Mass Spectrometry and Auger Electron Spectroscopy (AES) were used to study adsorption behavior of Te on "atomically clean" and As-passivated (112) surfaces. The surface kinetics of Te on the two different surfaces were analyzed, and an interface model is proposed that seem to suggest that nucleation on As-passivated surfaces lead to better epitaxy and subsequently produces CdTe layers of better crystallinity. High Resolution transmission Electron Microscopy (HRTEM) was employed to view the ZnTe/Si interface structure.

II. Methodology

The Lennard-Jones potential model [5,6] can describe adsorption phenomenon on clean surfaces. Gas molecules near surfaces experience attractive forces, which lead to adsorption. These forces are known to originate fundamentally from the electromagnetic interactions of the nuclei and electrons comprising the adsorbate-adsorbent system. Typically the nature of these interactions are best described by the principles of quantum mechanics [5,7,8]. It is assumed that, when tellurium molecule approaches the silicon surface, dispersive forces between Te_2 and the surface site causes interaction. This interaction and the associated energy change can be described by the Lennard-Jones (6-12) potential model [9]:

$$\phi(R) = -\frac{C_{LJ}}{R^6} + \frac{B_{LJ}}{R^{12}} \qquad (1)$$

Where R is the distance between the Te_2 and the surface site and C_{LJ} and B_{LJ} are the Lennard-Jones coefficients. Two curves can be expected for the case of Te_2 adsorption on a Si surface, one each, for physisorption and chemisorption. This is illustrated in the figure 1.

By definition, physisorbed Te_2 is attached to the surface in its molecular state. This assumption is true for all diatomic gases interacting with surfaces at low temperature [6]. Let the free energy of the Gas State of the Te_2 molecule is referenced as zero. As the molecule approaches the surface it experiences Van der Waal's forces. Upon physisorption, the change in energy at equilibrium separation (E_p) characterizes the minimum Energy State of the system. The equilibrium distance corresponding to the reaction coordinate will be equal to the sum of the Van der Waal's radius of Te_2 molecule and the effective radius of the Si surface site.

The situation is very different for chemisorption. Hypothetically, the Te_2 molecule dissociates prior to forming chemical bonds with the Si surface sites. This means that the reference energy E_{ref} has to be increased by the Te_2 dissociation energy, E_{diss} as indicated in figure 1. E_{diss} is equal to 2.677 eV per molecule [10]. As Te atoms in the dissociated state approach the surface, electronic redistribution creates bond formation. The system reaches an energy minimum at the chemisorbed state. This minimum energy corresponds to separation equal to the sum of the equivalent covalent radius for the Si surface site and for the Te atom. Therefore, the net energy change of the system from the "dissociated state" to the chemisorbed state is the bond energy per Te_2 molecule.

In terms of the activation energies, the Lennard-Jones potential model (figure 1) can be represented on the thermodynamic reaction coordinate for adsorption of gas molecules as illustrated in figure 2. It is noted that the barrier to adsorption is the activation energy of adsorption E_a, and it is referenced with respect to the gas state (E=0). The barrier to desorption is the activation energy of desorption E_d. E_p is the heat evolved during physisorption. By definition, E_c is the free energy change at chemisorption with respect to the gas state, and $E_c = E_{bond} - E_{diss}$. Notice for a monomer (monatomic molecule) $E_{diss} = 0$, and $E_c = E_{bond}$. E_{bond} is the net energy required dissociating the Si-Te bond. Consequently, from figure 1 & 2 we get,

$$E_{bond} - E_{diss} = E_c = E_d - E_a$$

and,

$$E_{bond} = \frac{1}{2}\left(E_d - E_a + E_{diss}\right) \tag{2}$$

A factor of 1/2 is included to express bond energy per atom. E_d is calculated using the measured desorption rates from experimental isotherms, E_a is calculated from the Langmuir's adsorption-desorption equilibrium condition.

The "activation energy" is related to the absolute rate constant of a given reaction. The experimental absolute rate constant (k) of a reaction, is typically given by the Arrhenius rate law [11]:

$$k(T) = A\exp\left(-\frac{E}{k_B T}\right) \tag{3}$$

Where, A is a constant known as the "frequency factor", E is the activation energy, k_B and T are the Boltzmann's constant and absolute temperature, respectively. Theoretical absolute rate constant of a reaction can be expressed in terms of the partition functions of the "activated complex" (Q_*) and the reactants (Q_c). It is given as:

$$k(T) = \frac{k_B T}{h}\frac{Q_*}{Q_c}\exp\left(-\frac{E}{k_B T}\right) \tag{4}$$

The general transition state theory was first applied to surfaces by Laidler et al. [12]. The calculation of absolute rate of reaction can be made using partition functions of the initial and activated states. Experimental isotherms from the surfaces can be used to calculate activation energies of adsorption and desorption. These activation energies are used to determine the surface Te-Si bond energy.

In this model Si surface effects and lateral interaction effects are neglected. First of these is the effect due to the surface heterogeneity. High index surfaces such as the (112) oriented Si is not very uniform in terms of the activities of the surface sites. Several step, kink, terrace and impurity sites are typically present which may alter the dominant adsorption mechanism. The Si-Te bond energy at different sites may therefore be different. Secondly, the influence induced by the interaction of nearest neighbor tellurium atoms on the surface would possibly change the Si-Te interaction energy, and hence the bond energy. Effects of the later situation would be small when the mean distance between Te atoms is large. This can be achieved by measuring

rates of reaction at low coverage. By measuring several isothermal desorption rates at temperatures adjacent to the maximum desorption peak would lead to a desorption energy relevant to that particular site. However, If several peaks corresponding to different sites overlap, then errors in estimating the desired bond energy could be considerable. If the Si-Te bond energy is considerably higher than the Te-Te lateral interaction energy, and the maximum desorption peak temperatures are resolvable, even when there is partial overlap, then both these effects would be less important.

III. Experimental

Samples were prepared in a molecular beam epitaxy machine (MBE) under an ultrahigh vacuum condition. The MBE system was equipped with standard analytical tools including Auger Electron Spectroscopy (AES), Mass Analyzer and Reflection High-Energy electron Diffraction (RHEED). Si wafers were first prepared in a hydrofluoric acid solution to get hydrogen terminated surface [13]. “Atomically clean" (112) Si surfaces were prepared in the growth chamber by desorbing hydrogen at 550^o C. As-terminated surfaces were obtained by heating samples between 550^o C to 580^o C under a stabilizing As_4 flux. Te-terminated surfaces were prepared by subjecting Te_2 flux on the “atomically” clean surfaces at three different temperature range, above 450^o C, between 450^o-350^o C and below 350^o C. ZnTe growth was performed by migration enhanced epitaxy (MEE) at a substrate temperature of 250^o C [14]. Surface polarity was studied by etching CdTe layers grown on ZnTe buffers [15].

Quantitative surface coverage (θ) measurements were made by AES in-situ the MBE system. A detailed quantitative surface analysis can be found in reference [16]. In this work all Te coverage measurements were made in the linear region $0 < \theta < 0.7$ ML. The intensity ratios for a monolayer was calibrated by first obtaining Auger standard signals from an “atomically” clean Si, and from a thick amorphous Te layer deposited on clean Si substrate. A series of Te (483 eV)/Si (92 eV) peak-to-peak intensity ratios were measured from surfaces with increasing Te coverage. A calibration curve of θ vs. intensity ratios was obtained by normalizing against the standard Te/Si ratio equivalent to one ML.

Temperature programmable desorption (TPD) spectroscopy was made by heating substrates with saturation Te coverage. Substrates were placed near (less than one inch) the mass spectrometer analyzer grid. A linear heating schedule of two degrees per Kelvin was employed.

IV. Bond Energy

Since (112) Si surface is composed of (111) terraces and (100) step edges, it is expected that this high miller index surface would possess more than one type of adsorption sites. The different adsorption sites can be inferred by observing various characteristics desorption peaks in the tellurium TPD spectrum shown in figure 3. At relatively low temperatures, $200° \leq T \leq 300°$ C, saturation coverage was found to be more than a mono-layer (ML). Below 200° C significant tellurium was found to adsorb as molecules.

A well resolved peak labeled α occurs at around 250° C, and several overlapping peaks appear between 500° C to 850° C. These peaks are labeled as, β_1 (629° C), β_2 (697° C) and β_3 (805° C). The α peak was not observed above 350° C or at Te coverage below one ML. The α

peak is thus identified as desorption of the physisorbed Te_2 molecules from a saturated Te-Si surface.

Multiple desorption peaks of figure 3 suggest that there are indeed different adsorption sites on the (112) Si surface. Winkler et al. [17] reported qualitatively similar TPD spectra for O_2 on (112)Pt. From their studies of desorption from (111) and (112) Pt surfaces the authors found that O_2 desorption from (112)Pt surface cannot be considered as a simple addition of desorption processes on (111) terrace sites and (100) step sites. Similar desorption behavior of H_2 from stepped Pt surfaces have been reported [18]. The effect of vicinality on the kinetics of adsorption has been studied by many authors [19]. These studies suggested that the rate of adsorption is typically increased in the presence of steps, and that the adsorbate binding energy is higher at the step-edge sites. It is thus reasonable to speculate that the β_1 peak originates from terrace sites, and the β_2 and β_3 peaks are associated with step and kink sites. In the present study β_1, β_2 and β_3 peaks appear in all desorption spectra from (112) Si regardless of the initial Te adsorption conditions. Hence it may be noted that the sticking probability of Te is approximately equal on all β sites. On a perfect (112) Si surface there are approximately two-third terrace sites, and about one-third step-edge sites. This proportionality is also reflected in the area under each curve in the TPD spectrum.

The activation energy (E_d) of desorption can be directly estimated from the TPD spectra using the Redhead equation:

$$\frac{E_d}{k_B T_m^2} = \frac{n\theta^{n-1}}{\beta_T}\kappa_n \exp\left(-\frac{E_d}{k_B T_m}\right) \qquad (5)$$

Where, T_m, n, κ_n, β_T are the maximum desorption temperature, order of the reaction, frequency factor (same as A), and the heating rate, respectively. To evaluate E_d the order of reaction n, and absolute rate constant K_d, must be determined.

Desorption rate constants $k_d(T)$, were determined from slopes of isothermal desorption rate data (IDR) (θ vs. time) of tellurium from Si surfaces at 826 K, 843 K, 868 K and 896 K. These temperatures were carefully chosen near the leading edge of the maximum desorption temperature peak (T_m). Tellurium coverage starts at t=0 at some initial value θ_o at a given temperature, and decreases asymptotically approaching an equilibrium value. The IDR data was linearized using Powell's method [20].

The order of the reaction n, was determined by using Powell's [20] graphical procedure of dimensionless parameters:

$$\ln\frac{\theta_o}{\theta(t)} = k_d(T)t \qquad \text{for n=1} \qquad (6a)$$

$$\frac{1}{(n-1)}\left[\frac{1}{\theta(t)^{n-1}} - \frac{1}{\theta_o^{\,n-1}}\right] = k_d(T)t \qquad \text{for } n \neq 1 \qquad (6b)$$

For each isotherm, n was evaluated by comparing the theoretical curves generated by the Powell's method with the experimental data. Comparison with theoretical curves suggested a second order desorption mechanism. An analysis by the Powell's method is presented in figure 4. The second order desorption process is well justified by the model chemical reactions of tellurium desorption from Si surfaces [21].

Having obtained the values of $k_d(T)$ and n, E_d can be calculated from eqn. 3 or eqn. 5. The resulting Arrhenius curve is shown in figure 5. The slope of $\ln k_d(T)$ vs. 1/T yields a desorption activation energy $E_d = 4.3 \pm 0.1$ eV, and the intercept gives the pre-exponential factor $A = 6 \times 10^{24 \pm 3}$ $ML^{-1} s^{-1}$. On the other hand, substituting all values in the Redhead equation (5) and evaluating E_d by iteration, we get a value of $E_d = 4.58 \pm 0.1$ eV. Thus estimates of E_d by two completely different experimental techniques yield very comparable values.

The activation energy of adsorption E_a in figure 2 is calculated from the Langmuir's adsorption-desorption condition. For a second order reaction we can write the Langmuir's rate of adsorption,

$$r_a = (1-\theta)^2 J e^{-\frac{E_a}{k_B T}} \qquad (7)$$

And the second order rate of desorption,

$$r_d = k_d \theta^2 \qquad (8)$$

And the thermodynamic absolute constant k_d, is given as:

$$k_d = \frac{k_B T}{h} \frac{Q_{**}}{(Q_a)^2} e^{-\frac{E_d}{k_B T}} \qquad (9)$$

Here Q_{**} and Q_a are the complete partition functions for the activated complex and adsorbate, respectively, and E_d is the activation energy of desorption.

At steady state, the net Te_2 (gas) flux (J) change near the Si surface is zero, thus $r_a = r_d$, and hence the surface coverage θ is constant. To calculate E_a, parameters J, k_d and θ were first determined. An atomically clean Si substrate held at a constant temperature of $T_{sub} = 823$ K was exposed to a Te_2 beam-equivalent-pressure (BEP) of 1.23×10^{-8} Torr. Setting the tellurium cell temperature to 487 K produced this BEP at the substrate location. The flux J near the substrate surface was estimated to be approximately 3.1×10^{12} molecules $cm^{-2} s^{-1}$ or 6.2×10^{12} atoms $cm^{-2} s^{-1}$. The substrate was held under J for 45 minutes to ensure equilibrium, and was immediately moved to measure θ on the surface. Auger peak-to-peak measurements on a set of three such surfaces yielded an average value of $\theta \approx 0.6$ ML. The desorption rate constant (k_d) for an initial coverage of $\theta_o \approx 0.6$ ML was estimated from the slope of the IDR data of θ vs.

time at T = 823 K. The rate constant was determined to be $k_d = 6.6 \times 10^{-3}$ ML^{-1}-s^{-1}. Next, a desorption rate of $r_d = 2.4 \times 10^{-3}$ ML-s^{-1} was calculated.

Substituting the above calculated values for J, θ and r_d, and using 1 ML = 8.3×10^{14} atoms cm^{-2} for a (112) surface, a value for the adsorption activation energy, $E_a = 50 \pm 10$ meV was determined. Finally, the Si-Te bond energy can be evaluated from the model equation 2. This evaluates to a bond energy of **E_{bond} = 3.46 ± 0.1 eV**. This result agrees remarkably well with the result reported by Oh and Grein [22]. They calculated the Si-Te bond energy on (001) Si substrates using quantum mechanical numerical method. These results are presented in Table 1.

V. Kinetic Analysis

It is of interest to know whether the Te atoms are mobile or localized on the surface, i.e. the surface mobility. The desorption rate constant given in eqn. 9 is rewritten below,

$$k_d = \frac{k_B T}{h} \frac{Q_{**}}{(Q_a)^2} e^{-\frac{E_d}{K_B T}} \qquad 10$$

The theoretical frequency factor, κ for a second order reaction, which is equivalent to the experimental frequency factor A, is simply given as:

$$\kappa = \frac{k_B T}{h} \frac{Q_{**}}{(Q_a)^2} \qquad 11$$

The partition function Q_{**} which lacks one degree of freedom (translational) can be written in as the products of its vibrational, rotational and translational partition functions. Since the "activated complex" in the precursor state is loosely bound to the surface, its partition function would be same as the gas state, except that it is confined in two dimensions. The third dimension of freedom simply leads to desorption. Thus using typical value [20] we get,

$$Q_{**} = Q_{vib} Q_{rot}^2 Q_t^2 = (1)(100)^2(1 \times 10^9)^2 = 1 \times 10^{22} \text{ cm}^{-2}$$

If we assume that the adsorbed state is mobile, then by choosing a typical value for the vibrational frequency normal to the surface $\nu = 6 \times 10^{12}$ s^{-1} [6, 9], we get for an upper limit of temperature at T = 1000K a value $Q_{vib} = 4.0$ in one degree of freedom. Since it is assumed mobile there are two degree of translational freedom. Again substituting typical values,

$$Q_a = Q_{vib} Q_t^2 = (4)(1 \times 10^9)^2 \approx 4 \times 10^{18} \text{ cm}^{-2}$$

On the other hand, if we assume that the adsorbate is immobile, the translational partition function will be unity. Then the Te atoms will be localized and vibrating in all directions, and Q_a can be expressed as [9]:

$Q_a = Q_{config} Q_v$

Where Q_{config} is the part of the total partition function Q_a that gives the total number of ways Te atoms can be arranged on the (112) Si surface sites. If we assume that Te bond to the surface tetrahedrally, than on the (111) type surface (terrace), a Te atom would bond with three hybrid bonds below. Therefore there are three surface Si atoms per site. On a (112) surface there are approximately 8.3 x 10^{14} cm^{-2} (equivalently one ML) Si atoms. Hence counting each site=3 Si atoms, we get approximately Q_{config} = 2.7 x 10^{14} cm^{-2} surface sites. Furthermore, since the Te atoms are rigidly bound to Si atoms, presumably with a 3.46±0.1 eV bond energy, the vibrational partition function can be approximated to unity. Thus, substituting values we get:

$$Q_a = Q_{vib} Q_{config} = (1)\ (2.7 \text{x} 10^{14}) \approx 2.7 \text{ x} 10^{14}\ cm^{-2}$$

Next, if we choose T = 1000K, an upper limit of temperature, we get,

$$\frac{k_B T}{h} = 2 \text{ x } 10^{13}\ s^{-1}$$

After substituting all values in the expression for κ in eqn. 11, we get:

$\kappa \cong 1 \text{ x } 10^{13}\ ML^{-1}\text{-}s^{-1}$ for the ***mobile*** case,
And
$\kappa \cong 2.77 \text{ x } 10^{21}\ ML^{-1}\text{-}s^{-1}$ for the ***immobile*** case.

Comparing these values with the experimentally determined frequency factor A = 6 x $10^{24\pm3}$ $ML^{-1}\text{-}s^{-1}$ it is clear that this frequency factor corresponds to the immobile adsorbed tellurium case. Therefore it is concluded that the tellurium adsorption on clean (112) Si surfaces is a second order process, where a molecule of tellurium dissociates into two atoms upon chemisorption. The bond energy at chemisorption is equal to 3.46 ± 0.1 eV. Finally, the surface diffusion of tellurium ad-atoms on the Si surface is negligible (immobile). This study suggests that up to a 0.6 monolayer coverage, tellurium adsorption is uniform and does not cluster. The situation of coverage between 0.6 and 1 ML is not clear and may be understood by considering the net charge differences at the interface.

VI. Nucleation and Interface Structure

To understand ZnTe nucleation and the microscopic interface structure of {112}ZnTe/Si, several adsorption experiments were carried out and adsorbed species on the Si surfaces were analyzed with AES. It was observed that Zn did not stick on atomically clean Si or on the As-passivated surfaces in the temperature range between 200°C and 600°C. Therefore ZnTe nucleation on either atomically clean or Te precursor Si surface initiates by the formation of Si-Te bonds. For the case of As-precursor Si surface, ZnTe nucleation is also expected to initiate by the formation of either Te-As or Si-Te bonds or both.

VII. Interface: Te-Precursor Surface

The most dramatic feature associated with the ZnTe growth on (112) Te- Si surfaces is the appearance of high density of twin defects (stacking faults) near the interface and in the bulk of the CdTe Layers. CdTe layers exhibited rough (faceted) surface morphologies. The ZnTe nucleation mechanism and subsequent interface structure can be discussed for two temperature

regimes indicated in the surface phase diagram of figure 6. When the Te-Si surfaces are prepared at temperatures above 450°C the Te surface coverage is less than a monolayer. It has been well established that at temperatures above ~500°C atomically clean Si surfaces can undergo large-scale structural rearrangement [23]. The rearrangement is enhanced when Si surfaces are vicinal, where large amounts of mass transport of the surface Si atoms occur leading to surface reconstruction, and at very high temperatures typically greater than 850°C step rearrangements leads to surface facets [24]. Under these circumstances Te ad-atoms can substitute the Si sites in the subsurface region.

In the case of (111)CdTe/(001)Si hetero-epitaxial structure, Wallis et al. [25] have observed the interface under a Z-contrast STEM and found evidence of Te atoms embedded as far as 3-4 monolayers from the surface into the Si substrate. In that case the interface comprised of a very thin layer of silicon-telluride template connecting the Si substrate with the ZnTe or CdTe overgrowth. For the same hetero-epitaxial structure, Sporken et al. [26] reported a model suggesting that the interfacial layers retain tetrahedral sp^3 bonding. The model describes the incorporation of Te atoms in the Si dimers on the (2x1) reconstructed (001)Si surface in a way that a Te atom replaces one of the two Si atoms in a dimer leaving an upward free ("dangling") bond. Hence incoming Cd or Zn atoms bond with the Te atoms thereby initiating a (111)B CdTe growth. This model was further evaluated by Oh et al. [22] using a quantum mechanical tight binding approach. Interface energy calculation was made for both, single and double stepped vicinal (001) Si surfaces. The calculated Si-Te bond energy per atom for single and double step Si surfaces were reported to be 3.522 eV and 3.497 eV, respectively. These calculated bond energies are very close to the Si-Te bond energy of 3.46 eV reported in this work.

In the present case of (112)ZnTe/(112)Si interface structure, a similar explanation can be given for the B-type ZnTe growth on Te-Si surfaces prepared at temperatures above ~500°C. With regards to the above described case of (001) Si surface, adsorption on (112) Si surfaces at temperatures above ~500°C would be such that some of the surface Si atoms would be substituted by the Te atoms. This would be possible if some of the surface Si atoms migrate to step edges and attach. This process can take place by the way of step bunching. Step bunching has been reported on vicinal (6° towards <011>) (111) Si surface for arsenic adsorption by Ohno et al. [27]. Since the adsoption probabilities of Te on clean (112) Si were approximately same for step and terrace sites, and the adsorbed tellurium atoms have very limited surface mobility, the ZnTe nucleation is equally likely on both sites. The adsorption of Te on terraces could possibly have two crystallographically equivalent configurations. Since at the interface a tetrahedrally coordinated ZnTe structure is expected and the underlying Si surface would retain its three-fold (111) symmetry, Zn exposure at the initial stage of MEE would generate randomly distributed nuclei that are mutually rotated with a 180° mirror symmetry. This state of affair is illustrated in figure 7. Subsequent ZnTe deposition would start growth of small islands formed by the lateral and vertical enlargement of these nuclei. Upon coalescence the 180° oriented islands will create twin domain boundaries in addition to twins and interfacial misfit defects that are generated during ZnTe lattice relaxation. Additionally the growth initiated from the step edges would combine with the growth at the terraces to give crystallographic facets. These facets would appear at the ZnTe surface and subsequently would be manifested on the CdTe surface.

As the temperature at which Te is adsorbed to prepare Te precursor surfaces is reduced, the surface mobility of the Te adatoms also diminishes. Hence the density of the terrace and edge nuclei as well as the density of the misoriented nuclei increases; thus the surface facet density is expected to increase. Furthermore, when the initial Te adsorption temperature is reduced below 500° C the tendency of replacing sub-surface Si atoms with Te also becomes less favorable. In

this case Te is expected to adsorb directly on top of the Si surface with one bond directed down and three bonds directed above. Thus, the ZnTe growth sequence of Si-Te-Zn--Te-Zn is expected. Clearly, this growth sequence would lead to an A-face ZnTe layer and subsequent CdTe deposition would also produce Cd terminated A-face layer as have been observed experimentally.

When the temperature at which the Te precursor surface is prepared is further reduced below 350°C, the tellurium surface concentration would increase to slightly in excess of a monolayer and Si-Te bonding become more disoriented leading to amorphous silicon telluride formation. This amorphous phase was also confirmed by RHEED. Further ZnTe followed by CdTe deposition would inherently cause polycrystalline growth with grossly rough surface as observed experimentally.

VIII. As Precursor Surface

The situation is significantly different for the case of As precursor (112) Si surface. Adsorption of As on (001) and (111) Si surfaces have been studied extensively [27, 28,29]. On a (111) Si surface it has been suggested that As atoms occupy the top sub-lattice sites by replacing the surface Si atoms. Patel et al. [30] measured the arsenic atom location using X-ray standing wave technique and found that the As atom in this surface sub-lattice site lie at 0.17Å above the un-relaxed bulk terminated (111)- Si plane. The As atoms are three-fold coordinated with the bottom Si sub-lattice atoms of the (111) bi-layer plane similar to the high temperature Te adsorption. The difference however is the presence of electron lone pairs on each As atom. This atomic configuration leads to a complete saturation of Si surface bonds thus yielding a nearly perfect surface passivation.

Arsenic adsorption on a clean (001) Si leads to the disruption of the surface reconstructed Si-Si dimers, and a monolayer of symmetric As-As dimer is added to the surface. Bringans et al. [31] reported detailed mechanism of As adsorption and bonding on a vicinal (001) Si surface. They reported that the As-As dimer direction on a vicinal (001) Si surface depends on the exposure to As and the surface temperature.

Arsenic adsorption on (112) Si has not been reported. However, LEED study of As adsorption at temperatures below 800°C on (111) Si mis-oriented by 12° towards $[\bar{1}\bar{1}2]$ direction reported by Ohno et al. [32] suggests step bunching consisting of a mixture of single and double step heights.

The (112) Si surface is very similar to the (111) Si mis-oriented by 12° in $<\bar{1}\bar{1}2>$ except the misorientation is 19.47°. Upon As adsorption the (112) Si surface also undergoes major rearrangement as evidenced by the increase in the background RHEED intensity followed by a (1x1) pattern of a stable passivated surface structure. Based on the above survey, the properties of the As passivated (112) Si surface is not expected to deviate from those of the highly vicinal (111) surfaces in any significant way. Insofar, we can expect, similar to the vicinal (111) Si surfaces, the As atoms would occupy the top (111) terrace sub-lattice Si sites accompanied with step bunching. It is noted that adsorption of As at the edge site may not be energetically favorable. This is because, when As is adsorbed, the (112) Si surface is expected to conform to non-primitive configuration [33] with the exception of the top Si atoms being replaced by As atoms, such that, all As atoms are three-fold coordinated to enforce a tetrahedral bonding. The edge Si atoms are now from the lower half plane of the top bi-layer, and possess two free bonds per Si atoms lying in the (111) plane. The As passivated (112) Si surface configuration

would present a highly passivated surface and inhibit ZnTe nucleation on terraces at the initial stages of the growth. Therefore with subsequent exposure to Te and Zn during MEE would start growth by nucleating ZnTe unit cells via Si-Te bonds that are initiated at the step edges as described below.

IX. ZnTe Nucleation Model On As: (112) Si Surfaces

Tellurium adsorption studies were made to understand the initial stages of ZnTe nucleation process on the As-precursor (112) Si surfaces. As-precursor surfaces were subjected to Te flux for 1 minute at various temperatures between 250°C and 600°C. Auger measurements from these tellurium surface revealed that significantly less amounts of Te stick on As-precursor (112) Si surfaces compared to those of the clean Si surfaces. The auger peak to peak intensity of the Te-486 LMM line increased with the increase in the sample temperature suggesting that surface concentration of Te increases at higher temperature. This may be indicative of As displacement by Te at elevated temperatures. The surface coverage of Te on the As-passivated Si surfaces at 250°C (ZnTe growth temperature) was assessed by monitoring the ratio of the Te (486eV) to Si (92eV) auger peak to peak intensities. This ratio was compared with the Te/Si ratio obtained from the Te adsorbed at 250°C on clean Si surfaces under the same conditions. It was found that the Te saturation coverage (θ_{max}) on an As precursor Si surface was near 0.2ML, where as, θ_{max} on a clean (112) Si surface was slightly higher than a ML. This substantial decrease in θ_{max} clearly suggests that the As-precursor surfaces be extremely passivated.

The highly passivated nature of the As-precursor Si surface and low Te θ_{max} suggest that the incident Te dimers on terraces would have to migrate to the edges and attach to the exposed two fold coordinated Si dimers along the $[0\bar{1}1]$ direction. This is expected because the bond strength of Si-As on the (111) type Si surface is 4 eV [34], where as, the Si-Te bond strength on the similar type surfaces is 3.46 eV. Energetically, displacement of As atoms bonded to Si by the Te atoms is less favorable particularly at low temperatures. On the other hand, the As-Te bond strength is expected to be significantly smaller than both Si-As and Si-Te bond strength, thus any Te adsorbed to As will readily evaporate. Furthermore, if Te were to adsorb on top of the As passivate terrace sites the Te surface coverage would have been much higher than the coverage measured experimentally. It was stated that on a (112) Si surface the distribution of terrace and edge sites is two-third and one-third respectively. Similar site distribution is expected on the As-precursor (112) Si surface because the As adsorption lifts the (2x1) reconstruction from the clean (112) Si surface, and leaves an un-reconstructed (1x1) surface. Therefore, ideally, about one-third monolayer of Te would saturate all step edge sites. Hence a Te coverage of 0.2 MLs on As-precursor surfaces suggest that the step edges be only partially occupied.

Careful examination of the RHEED patterns from the Te adsorption on As-Si surfaces revealed the appearance of 1/3 diffraction order when the electron beam was incident in the $<\bar{1}\bar{1}2>$ with a 30° azimuthal rotation. This suggests that a periodic array of Te atoms bond to the step sites that are displaced by $3a/\sqrt{3}$ lattice distance in the $[0\bar{1}1]$ direction. When the electron beam is incident in the $<0\bar{1}1>$, it is observed that the Te adsorption leads to an enhancement of the terraces with a threefold decrease in the streak spacing. This indicates that the (001) steps have tripled perhaps by step bunching. Next, when Zn shutter is opened with Te shutter being closed, the RHEED pattern in the $<\bar{1}\bar{1}2>$ azimuth depicts distortion with an increase in the background intensity suggesting a roughening of the surface. The RHEED

observations can be explained as follows. Since the edge Si atoms are from the bottom sub-lattice of the top bi-layer these edge atoms possess two free bonds lying in the (111) plane. Upon the Si-Te bond formation at the step edges, the two hybridized free bonds on each Te atom would lie on a plane which is orthogonal to the (111) plane, thus directing one bond normal to the [111] terrace and the other below onto the adjacent lower terrace. Subsequent exposure to Zn during MEE initiates ZnTe nucleation at these edge sites by the formation of Zn-Te bond above and As-Zn bond below. The growth is expected to proceed uniformly in the lateral direction in a step-flow mode. RHEED observation during MEE indicated two-dimensional growth for several MEE periods. However, during each Zn exposure RHEED observation in the $<\bar{1}\bar{1}2>$ direction indicated the appearence of facets as seen by the arrowhead type features superimposed on the RHEED pattern. Further, during each Te exposure these features disappeared by displaying intense RHEED streaks. These RHEED features can be attributed to the tetragonal distortion at step edges, perhaps originating from the differences in the bond lengths between Zn-Te and Zn-As and Si-As. When Zn shutter is opened for the first time the incident Zn atoms on the Te:As:Si surface migrate to the step edges and bonds to Te above and As below thereby inducing a tetragonal distortion. A schematic illustration of ZnTe nucleation is shown in figure 8. It can be seen that this growth mechanism would lead to a Te terminated B-face growth.

The interface structure of ZnTe/As/Si(112) thus formed would have to accommodate the misfit by forming a periodic array of misfit dislocations at the interface preferably at the step edges. Additionally, a tilt angle between the ZnTe layer and the substrate is also expected. The misfit between Si and ZnTe is 12.4%. For an edge type or 60° type misfit dislocation array the misfit spacing is expected to be 31.4 Å or 15.7 Å, respectively [35]. However, HRTEM shown in figure 9 suggest that the misfit spacing is 25 Å, and selected are electron diffraction yields a 2° ZnTe layer tilt with respect to the Si surface. Since the width of a single terrace lattice unit (d_{TLU}) of (112) Si is equal to 7.76 Å, a triple step bunched surface would give about 23 Å between the step edges; a better fit for the observed misfit spacing. Furthermore, for a triple stepped surface the tilt angle of the ZnTe/As/Si interface can be estimated by considering the interface geometry. Three (111) ZnTe bi-layers are needed to stack on each (111) Si terraces. Since ZnTe lattice spacing in the <111> direction, d_{111}^{ZnTe} is 3.52 Å and is larger than the Si lattice spacing of d_{111}^{Si}=3.14 Å in the same direction, the difference in the height will cause a tetragonal distortion near the step edges thus causing a misfit dislocation. The difference in the height will be equal to $3(d_{111}^{ZnTe} - d_{111}^{Si})$= 1.14Å. As a result the ZnTe (111) terraces would have to rotate in the $<\bar{1}\bar{1}1>$, thereby producing an angle θ_t. The tilt angle is calculated as follows,

$$\theta_t = \tan^{-1}\left(\frac{1.14}{3d_{TLU}}\right) = 2.8°$$

If we take distortion due to arsenic at the interface we get θ_t=2.3°, again a better fit with the observed tilt angle.

Conclusions

It is concluded that ZnTe epitaxy on an As-terminated Si surface initiates at the step edges. The resultant CdTe overgrowth is usually of good crystallinity with excellent surface morphology. The crystallographic surface polarity is always B-type. ZnTe growth on "atomically" clean Si or on Te-terminated Si surfaces is dominated by terrace nucleation. The crystallographic surface polarity depends on the temperature at which the Si surfaces are

exposed to Te_2 flux. Te_2 exposure at temperatures above 500° C lead to B-type growth, and below 450° C gives A-type growth. Additionally, absence of As passivation typically produces CdTe layers with grossly rough surface morphologies. CdTe/ZnTe layers deposited on Te-teminated Si usually exhibits high density of stacking faults and other defects.

Acknowledgements

The support and assistance provided by Dr. J. Dinan of NVESD is greatly appreciated. The author also wishes to thank Dr. Yan Xin and Prof. Sivananthan of UIC microphysics lab for HRTEM work and interesting discussions.

References:

1. T. J. de Lyon, O. K. Wu, J. A. Roth, S. M. Johnson, and C. A. Cockrum, Appl. Phys. Lett. 63, 818 (1993).
2. R. Sporken, M. D. Lang, J. P. Faurie, and J. Petruzzello, J. Vac. Sci. Technol. B 9, 1651(1991)
3. R. Sporken, M. D. Lang, C. Masset, and J. P. Faurie, Appl. Phys. Lett. 57, 1449(1990).
4. A. Million, N. K. Dhar, and J. H. Dinan, J. Cryst. Growth, 159, 76 (1996); N. K. Dhar et al., J. Vac. Sci. Technol., B14, 2366 (1996).
5. A. D. Crowell, "The Solid-Gas Interface", E. A. Flood, Ed., Vol 1, Marcel Dekker, Inc., pp 175 (1967).
6. A. W. Adamson, "Physical Chemistry of Surfaces", John Wiley & Sons (1997).
7. Benjamin Chu, "Molecular Forces", Interscience Pub., John Wiley & Sons, (1967).
8. A. P. Sutton and R. W. Balluffi, "Interfaces in Crystalline Materials", Oxford Science Pub., Clarendon Press, Oxford (1995).
9. M. W. Roberts and C. S. McKee, "Chemistry of The Metal-Gas Interfaces", Clarendon Press, Oxford, pp305 (1978).
10. K. P. Huber and Herzberg, "Molecular Spectra and Molecular Structures: Constants of Diatomic Molecules", Van Nostrand Reinhold Co., (1979).
11. K. J. Laidler and H. Eyring, "The Theory of Rate Processes", Int'l Chem. Series, McGraw-Hill, Ney York, 1st Ed., (1941).
12. D. M. Bishop and K. J. Laidler, J. Chem. Phys., 42, 1688 (1965).
13. D. B. Fenner, D. K. Biegelsen, and R. D. Bringhans, J. Appl. Phys., 66, 419 (1989).
14. N. K. Dhar et al., J. Vac. Sci. Technol., B14, 2366 (1996).
15. W. J. Everson, C. K. Ard, J. L. Sepich, B. E. Dean, G. T. Neugebauer, and H. F. Schaake, J. Electron Mater., 24, 505 (1995).
16. L. V. Phillips, L. Salvati, W. J. Carter, and D. M. Hercules, "Quantitative Surface Analysis of Materials", ASTM STP 643, N. S. McIntyre, Ed., American Society for Testing and Materials, pp. 47-63, (1978).
17. A. Winkler, X. Guo, H. R. Siddiqui, P. L. Hagans, and J. T. Yates, Jr., Surf. Sci. 201, 419 (1988).
18. F. Zera and G. A. Somraj, "Hydrogen effects in Catalysis- Fundamentals and Practical Applications, Z. Paal and P. G. Menon, Eds., Marcel Dekker, N.Y., pp427 (1988).
19. H. Wagner, "Solid Surface Physics", G. Hohler, Ed., Springer-Verlag, Berlin, Heidelberg, N. Y. (1986).
20. A. A. Frost and R. G. Pearson, "Kinetics and Mechanism", 2nd Ed., John Wiley & Sons, N. Y., pp23 (1961).
21. N. K. Dhar, N. Goldsman, and C. E. C. Wood, To be published.
22. J. Oh and C. H. Grein, J. Cryst. Growth (In press).
23. Y. J. Chabal, J. E. Rowe, and S. B. Christmas, Phys. Rev. B 24, 3303 (1981).

24. A. A. Baki and L. J. Whitman, J. Vac. Sci. Technol., A 13, 1469 (1995).
25. Personal conversation with Prof. S. Sivananthan, work of wallis et al.
26. R. Sporken, Y. P. Chen, S. Sivananthan, M. D. Lang, and J. P. Faurie, J. Vac. Sci. Technol. B 10(4), 1405 (1992)
27. T. R. Ohno and Ellen D. Williams, Appl. Phys. Lett., 55, 2628 (1989).
28. M. A. Olmstead, R. D. Bringhans, R. I. G. Uhrberg, and R. Z. Bachrach, Phys. Rev. B 34, 6041 (1986).
29. R. I. G. Uhrberg, R. D. Bringhans, M. A. Olmstead, and R. Z. Bachrach, Phys. Rev. B 35, 3945 (1987).
30. J. R. Patel, J. A. Golovchenko, P. E. Freeland, and H. J. Gossmann, Phys. Rev. B, 36, 7715 (1987)
31. R. D. Bringans, D. K. Biegelsen, and L. E. Swartz, Phys Rev. B, 44, 3054 (1991).
32. T. R. Ohno and Ellen D. Williams, J. Vac. Sci. Technol., B 8(4), 874 (1990).
33. R. Kaplan, Surf. Sci., 116, 104 (1982).
34. M. Zinke-Allmang, L. C. Feldman, J. R. Patel, and J. C. Tully, Surf. Sci., 197, 1 (1988).
35. Booker et al., J. Crystal Growth., 45, 407 (1978).

Table 1: Comparison of Si-Te bond energies on (112) and (001) Si substrates.

	Energy per Atom (eV)
***SL SC**	**3.522**
***DL SC**	**3.497**
This Work	**3.46**

* J. Oh and C. H. Grein, J. Of Cryst. Growth
The calculation in the above reference was based on extended bond orbital approximation and approximated moments methods. The two values are based on single layer step (SL) and double layer step (DL) structures.

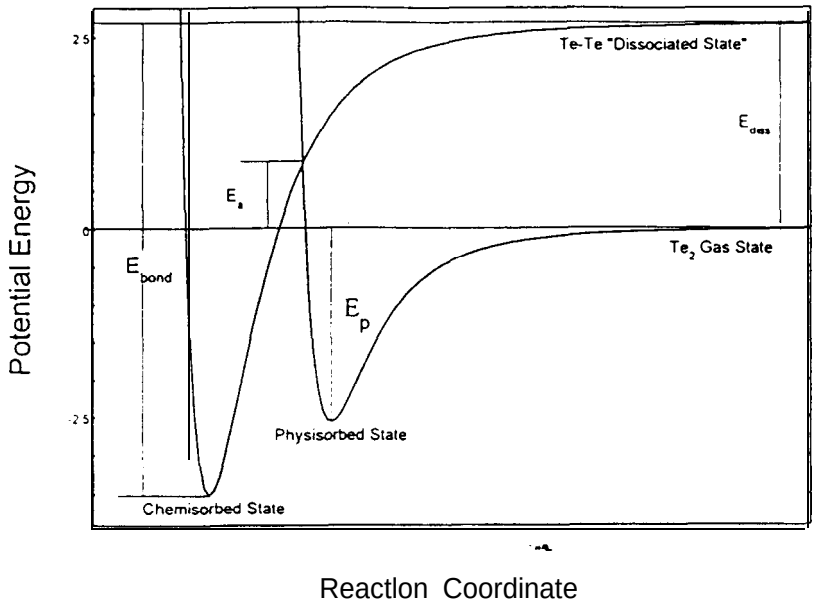

Figure 1 Lennard-Jones potential model for adsorption.

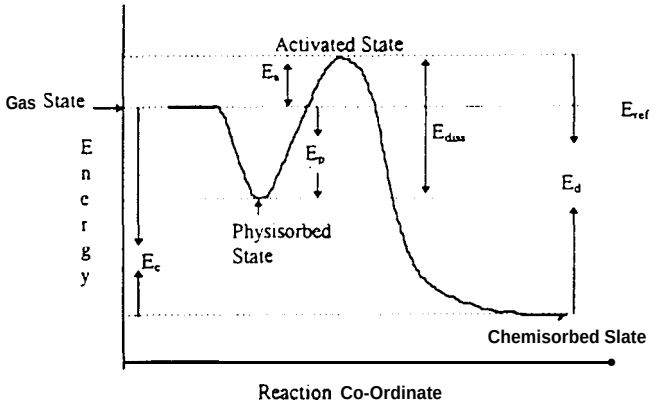

Figure 2 Energy diagram of Te_2 adsorption on a clean Si surface.

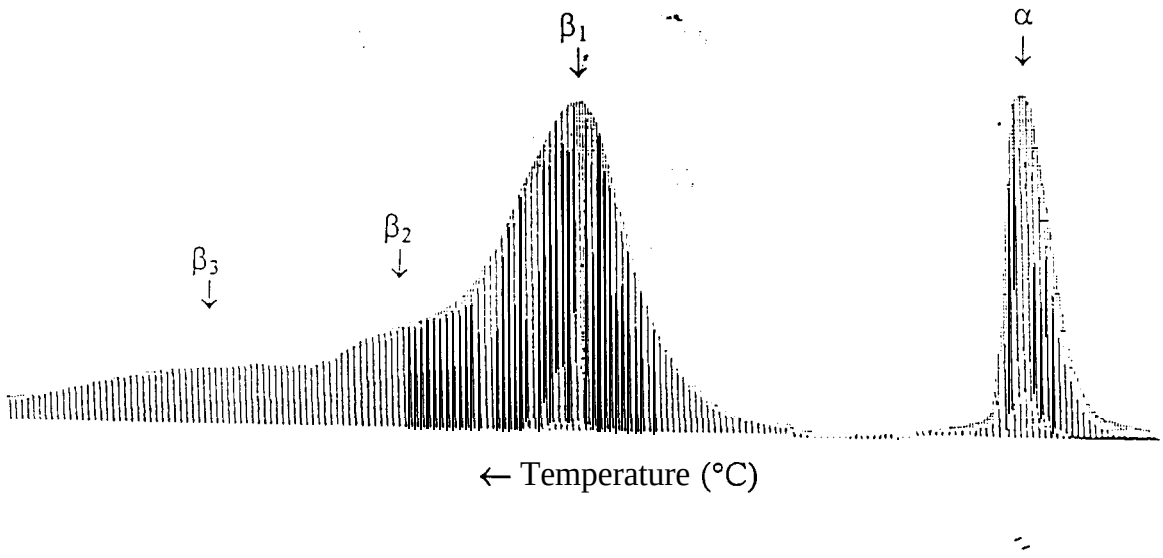

Figure 3 Temperature programmed desorption spectrum of Te_2 from (112) Si surface.

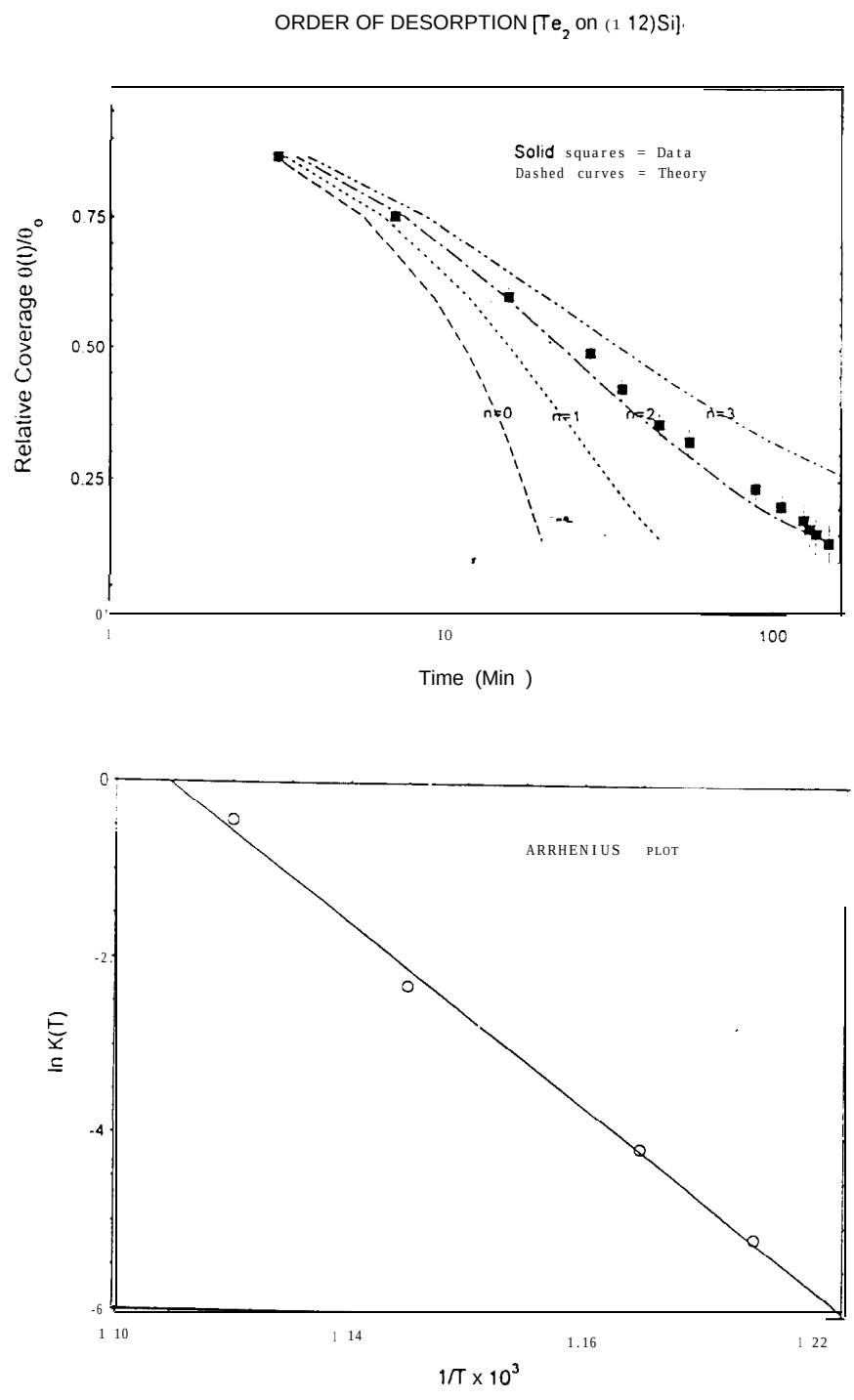

Figure 4 Top: Determination of the order of desorption using the Powell's method.

Figure 5 Bottom: Arrhenius plot of rate constants vs. reciprocal temperature to determine activation energy for Te desorption from (112) Si.

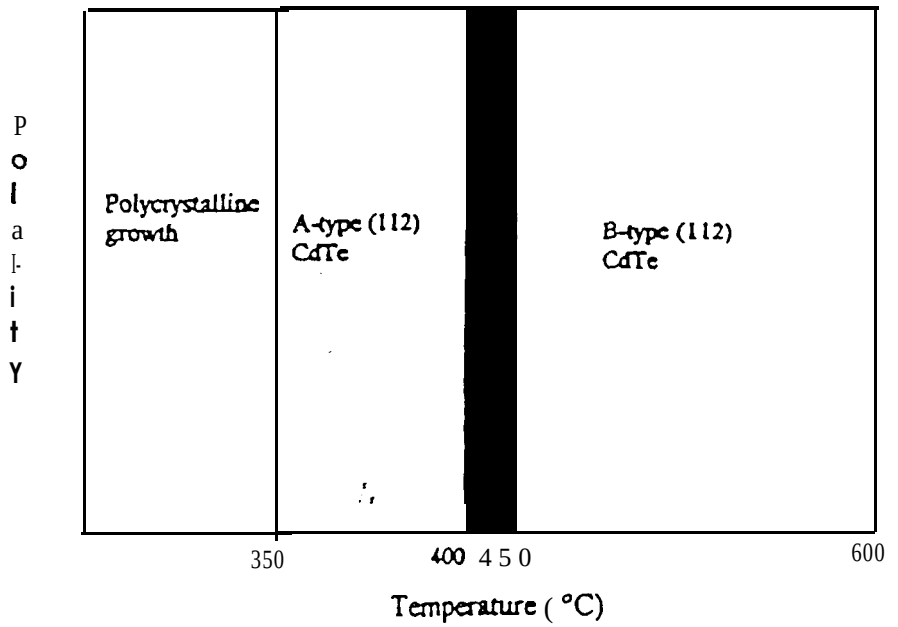

Figure 6 Surface phase diagram of crystalligraphic polarity ?. CdTe deposited on Te-terminated (112) Si surfaces.

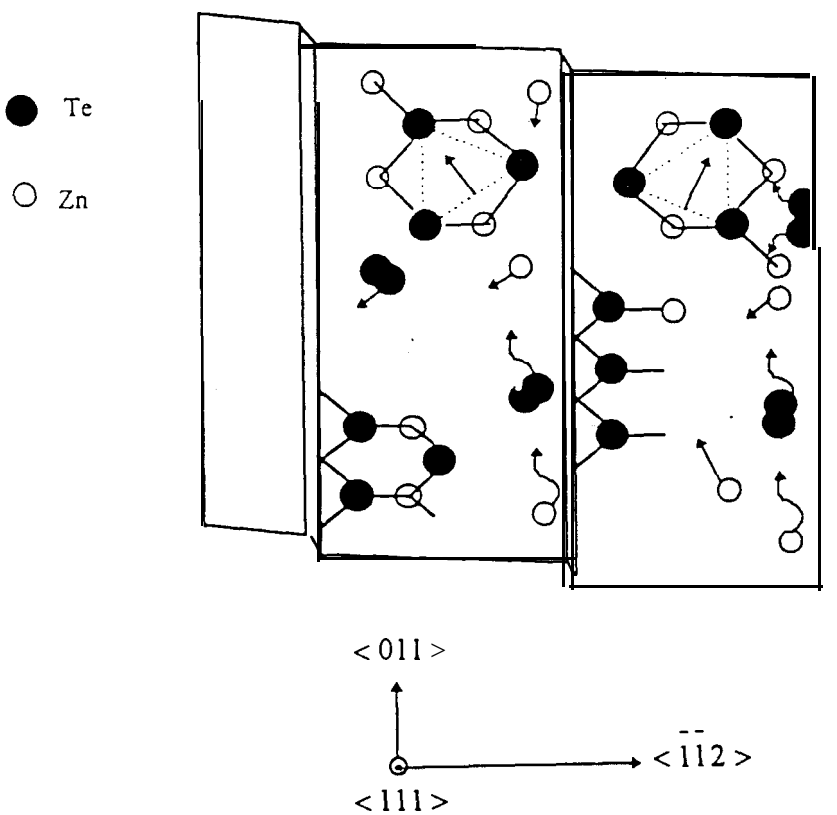

Figure 7 A schematic illustration of ZnTe nucleation on Te-terminated (112) Si.

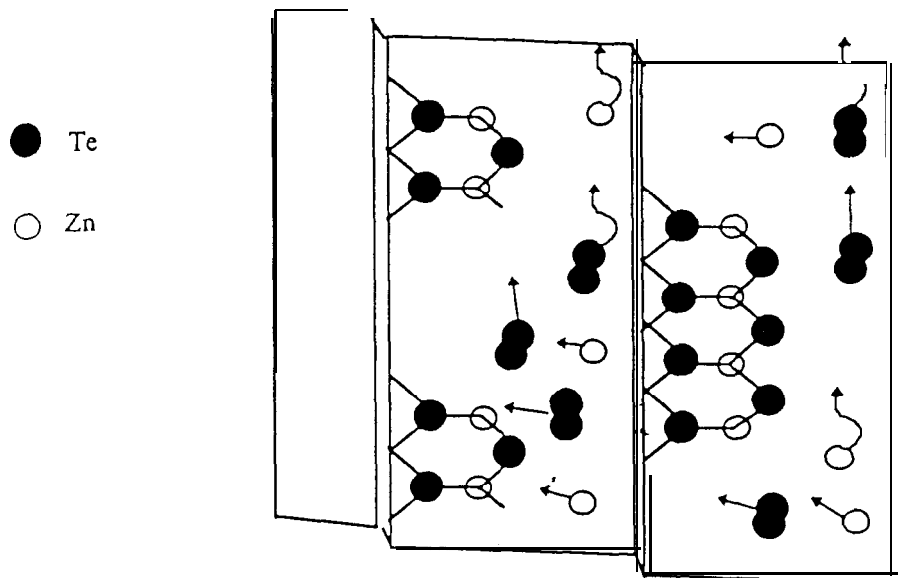

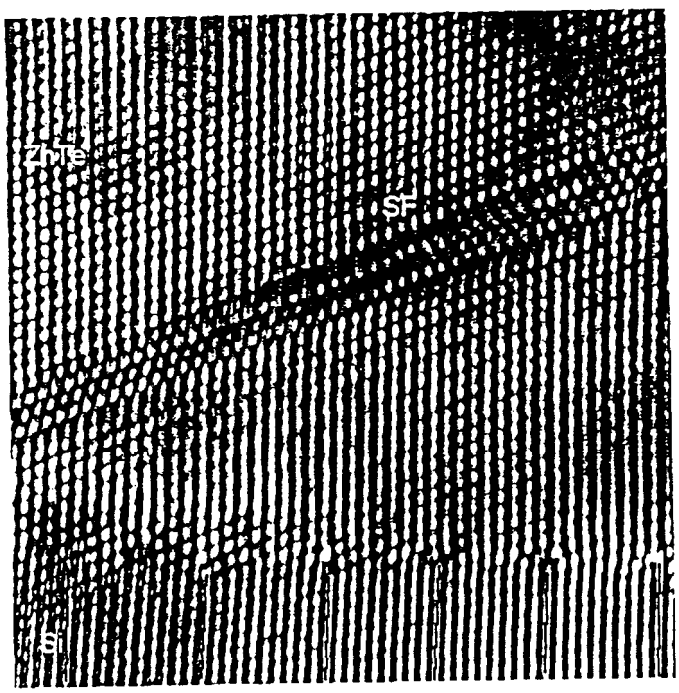

Figure 8 A schematic illustration of ZnTe nucleation on As-terminated (112) Si.
Figure 9 HRTEM image of ZnTe/As/Si interface showing the misfit spacing of **25Å.**